Universality behaviors and fractal dimensions associated with M-furcations

Shau-Jin Chang and John McCown*
Department of Physics, University of Illinois at Urbana—Champaign, 1110 West Green Street, Urbana, Illinois 61801
(Received 23 August 1984; revised manuscript received 28 January 1985)

We study the universality behavior and scaling property associated with an arbitrary M-furcation fixed point in a one-dimensional iterative map. We use both the direct-search method and the renormalization-group method to evaluate the fixed-point function $f^*(x)$ and the universal constants α and δ. The agreement between these two methods is very satisfactory. The basin of attraction of $f^*(x)$ forms a nearly self-similar Cantor set. We use this approximate self-similarity property to compute the capacity and the information dimensions of the attractor. We summarize M-furcation results for all $M \leq 7$ basic cycles in several tables.

I. INTRODUCTION

The one-dimensional iterative map[1–3]

$$x_{n+1}=f(x_n)$$

forms the simplest deterministic system which gives rise to chaotic behavior. It also reveals many interesting phase-transition phenomena as the system becomes chaotic.[3,4] In addition to its rich structure, the iterative map also appears naturally in many branches of physics such as condensed matter physics,[5] fluid physics (turbulence in particular),[6] accelerator physics,[7] and others.

Transition to chaos is one of the outstanding problems in turbulence. Many processes appear to be important as a fluid on its way to chaos: onset of instability, period doubling, quasiperiodicity, period locking, intermittency,[8] etc. Some of the processes involve several relevant degrees of freedom and are intrinsically multidimensional. These multidimensional behaviors cannot be imitated in a one-dimensional map. On the other hand, we can understand certain aspects of the period-doubling and the intermittency phenomena by studying one-dimensional map. Feigenbaum has investigated the universality behavior of period doublings in one-dimensional maps.[3] Loosely speaking, intermittency describes the fact that the total volume occupied by the small vortices goes to zero as the vortex size goes to zero. Empirically, the space occupied by these small vortices can be described as a fractal with a fractal dimension ~ 2.5. If we look at a given volume in a fluid, the vortices will appear and disappear intermittenly. Hydrodynamics intermittency described above occurs for a range of parameters. In a one-dimensional map (1D), "intermittency" describes the short interruptions of an otherwise approximately periodic behavior. Instead of appearing for a continuous range of control parameter, the intermittency in a 1D map occurs only near the onset of tangent bifurcations. The other aspect of the hydrodynamics intermittency, namely, the realization of a fractal, also occurs in the one-dimensional iterative system: As we change a control parameter in $f(x)$, the system can go through a sequence of M-furcations and become chaotic (Feigenbaum-type transition). At the transition point, the basin of attraction also becomes a fractal. The analog described here is very crude. The fractal attractors in 1D maps occur only at isolated (but infinite in number) parameter values while, as mentioned earlier, the hydrodynamics intermittency occurs over a range of control parameter. This difference is probably related to the fact that we work on a 1D system. Nevertheless, we hope that, by studying the fractals in 1D maps, we may gain some insights for understanding the fractals in the hydrodynamics intermittency.

In this paper, we present a systematic study of all one-dimensional M-furcation transitions and their associated attractors with basic cycles $M \leq 7$. We obtain the critical exponents both numerically, and by renormalization-group calculations. We also obtain the fractal dimensions associated with these attractors. It is our hope and expectation that a thorough study of the simple system will teach us how to handle real turbulence in the future. A summary of our results has appeared previously.[9]

In Sec. II we give a review of Feigenbaum universality behavior associated with bifurcation, and then extend it to include arbitrary M-furcations. In particular, we work out the trifurcation in details. In Sec. III we study the behavior of an M-furcation transition by a direct numerical search of the associated M^n-cycles. In Sec. IV we obtain the universal behavior of M-furcations by renormalization-group calculations. It is pleasing to see that the results in Secs. III and IV agree perfectly with each other. In Sec. V we compute the fractal dimensions associated with the M-furcation attractors. We include some of the technical results in the Appendixes.

II. UNIVERSAL BEHAVIOR ASSOCIATED WITH AN ARBITRARY U SEQUENCE

Metropolis, Stein, and Stein discovered the universality of the U sequence for single-hump one-dimensional maps.[10] Feigenbaum made the important discovery that all single-hump one-dimensional maps with quadratic maxima have the same universality behaviors near the infinite bifurcation (2^n-cycle) limit.[3,11] He showed that one may understand this universal behavior quantitatively by a renormalization-group analysis. We can summarize some of the important behaviors as follows.

(1) The U sequence[10] P_n for a 2^n-cycle can be defined iteratively via the $*$ product[12] as

$$P_{n+1}=P_n * R \equiv P_n \cdot Q \cdot P_n \ , \tag{2.1}$$

where $Q \equiv R$ or L depending on whether the number of R's in P_n is even or odd. We may express P_n symbolically as $R(*R)^{n-1}$.

(2) The control parameter a_n associated with the 2^n-cycle approaches the limit a_∞ geometrically, i.e., at large n, we have

$$a_n \equiv a_\infty + \text{const}/\delta^n \tag{2.2}$$

or

$$\delta = \lim_{n\to\infty} \left[\frac{a_n - a_{n-1}}{a_{n+1}-a_n} \right] = \text{const} \ . \tag{2.3}$$

For the bifurcation sequence, $\delta = 4.669\,202$ is a universal number, but a_∞ is not.

(3) We choose the parametrization $f(x)$ of the map such that it has its peak at $x=0$. Then, the function

$$f_n(x) \equiv f_{n-1} \circ f_{n-1} \equiv f^{2\uparrow n}(x)$$

at a_∞ is self-similar near $x=0$ at large n. Indeed, for a properly chosen scaling factor

$$\alpha = -2.502\,908 \ ,$$

the limit

$$f^*(x) = \lim_{n\to\infty} [\alpha^n f_n(x/\alpha^n)] \tag{2.4}$$

exists and obeys the functional relation

$$\alpha f^{*2}(x/\alpha) = f^*(x) \ . \tag{2.5}$$

The function $f^*(x)$ is unique up to a trivial scale transformation, and is independent of the detailed behavior of $f(x)$. We usually fix the scale of $f^*(x)$ by $f^*(0)=1$.

(4) In the neighborhood of the universal function f^*,

$$f(x) = f^*(x) + \delta f(x) \ , \tag{2.6}$$

the operation of (2.5) gives

$$\alpha f^2(x/\alpha) = f^*(x) + \delta f'(x) \ , \tag{2.7}$$

where $\delta f'$ is related to δf via

$$\delta f' = \Lambda\, \delta f + O((\delta f)^2) \ . \tag{2.8}$$

Of all the eigenvalues of Λ, only one eigenvalue has a magnitude larger than 1. This eigenvalue is δ. All other eigenvalues have magnitudes smaller than 1. According to critical phenomena terminology, these other eigendirections are irrelevant. One can use relations (2.5)–(2.8) to compute f^*, α, and δ.

To see the generalization of Feigenbaum universality behavior from a bifurcation sequence (2^n-cycles) to an arbitrary M-furcation sequence (M^n-cycles), we work out the period tripling in details. For definiteness, we consider the map

$$x_{n+1} = -a - x_n^2 \equiv f(x_n) \ . \tag{2.9}$$

To within a trivial scaling, map (2.9) is identical to map (3.1) to be studied in Sec. III. The advantage of the present form is that the quadratic term has a fixed coefficient. We can see the tangent bifurcation even in the basic 1-cycle. Map (2.9) has no basin of attraction for $a > 0.25$. At $a=0.25$, the map develops a tangent bifurcation for the basic 1-cycle [Fig. 1(a)]. As a decreases, this basic 1-cycle goes through the superstable stage at $a=0$ [Fig. 1(b)], becomes unstable at $a=-0.75$, and is followed by a sequence of bifurcations. As we increase $-a$ further, we go through an infinite number of different cycles and finally becomes a single chaotic band at $a=-2$ [Fig. 1(c)]. Beyond $a=-2$, there are no more stable attractors. We may view this whole region, $-2 < a < 0.25$, as the window of stability associated with the 1-cycle.

Within this 1-cycle window, a 3-cycle window appears and disappears. Other than the bifurcation phenomena, the 3-cycle window is probably the most dominant feature of the single-hump map. The easiest way to see the 3-cycle window is to look at the map $f^3(x)$. In Fig. 2 we see the tangent bifurcation at $a=-1.75$ signaling the first appearance of 3-cycles [Figs. 2(a) and 2(b)], the superstable 3-cycle at $a=-1.754\,878$ [Figs. 2(c) and 2(d)], and three chaotic bands at $a=-1.790\,327$ describing the end of the 3-cycle window [Figs. 2(e) and 2(f)]. We can see the similarity between the 3-cycle window and the original 1-cycle window.

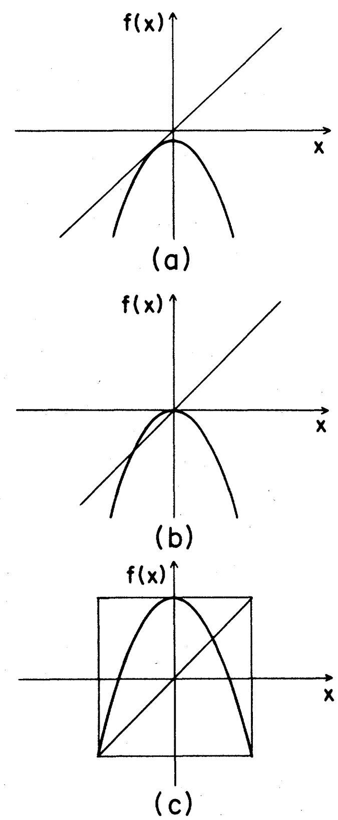

FIG. 1. Window of stability for map (2.9). (a) First appearance of stable 1-cycles through a tangent bifurcation at $a=0.25$. (b) Superstable 1-cycle at $a=-0.75$. (c) Chaotic band at $a=-2$ describing the end of the 1-cycle window.

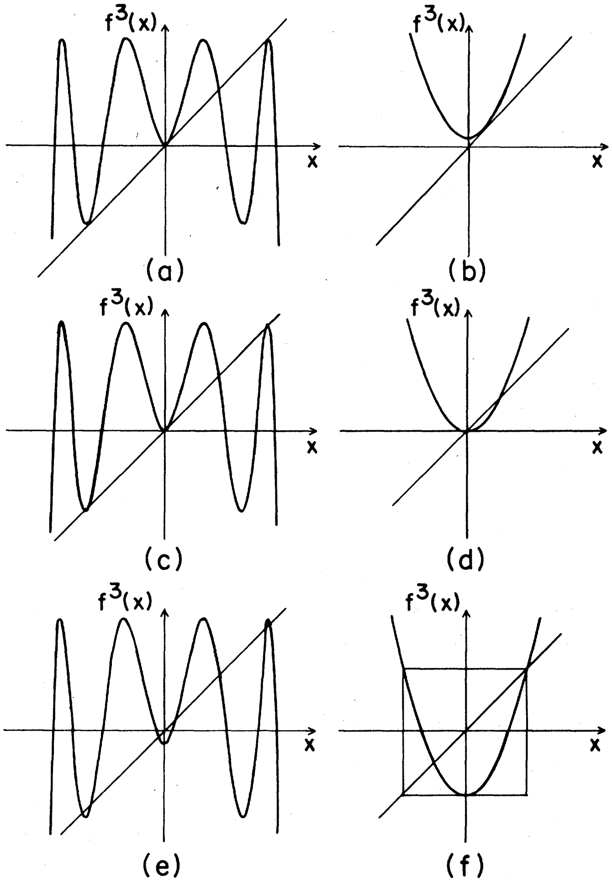

FIG. 2. 3-cycle window of stability for map (2.9). (a) First appearance of 3 cycles through tangent bifurcations at $a=-1.75$. (b) Enlarged center part of (a). (c) Superstable 3-cycle at $a=-1.754\,878$. (d) Enlarged center part of (c). (e) Chaotic 3-cycle bands at $a=-1.790\,327$ describing the end of the 3-cycle window. (f) Enlarged center of part of (e) containing the middle chaotic band.

If we look carefully, we can see the 9-cycle window inside the 3-cycle window, the 27-cycle window inside the 9-cycle window, etc. Since there is only one 3-cycle in a single-hump map, there are no ambiguities to find these windows. However, when we search for M-furcation windows associated with a 5-cycle or above, we need a more precise description of these cycles and their windows.

A precise way to describe an M-furcation is through the U sequence. In the case of trifurcation, the basic 3-cycle has the U sequence $U=RL$. It is easy to verify that the 9-cycle mentioned earlier has the U sequence $U=RL\underline{L}RL\underline{R}RL$. We underline the L and R in the U sequence to indicate that these form the U sequence of $f^3(x)$ as we observe the map every third time. Between these observations, the map behaves approximately as the original 3-cycle with $U=RL$. The sequence associated with $f^3(x)$, LR, is the original U sequence with L and R interchanged. This interchange of L and R is due to the fact that the map f^3 near the center is inverted. Since $f'(x)<0$ on the right of the peak, we always encounter the inversion if the U sequence of the original map contains an odd number of R. We can write down the U sequences and the parameters a_n associated with the superstable 3^n-cycles of the trifurcation series as

3	RL	$-1.754\,877\,666$
9	$RLLRLRRL\equiv P_2$	$-1.785\,865\,645$
27	$P_2RP_2LP_2\equiv P_3$	$-1.786\,429\,857$
81	$P_3LP_3RP_3\equiv P_4$	$-1.786\,440\,066$
$\cdots$	$\cdots$	$\cdots$
∞		$-1.786\,440\,255.$

This sequence was first studied by Derrida *et al.* As we have shown in Figs. 1 and 2, this sequence is self-similar, and gives a Feigenbaum-type fixed point with a new set of universal constants

$$\alpha=-9.277\,341\ , \tag{2.10}$$

$$\delta=5.524\,703\times 10^1 \tag{2.11}$$

and a new universal function $f^*(x)$ obeying

$$\alpha f^{*3}(x/\alpha)=f^*(x)\ . \tag{2.12}$$

The factor α describes the scaling needed to bring $f^{*3}(x)$ into $f^*(x)$. A negative α indicates that the map f^{*3} is inverted. See Fig. 2 for a qualitative realization.

We can generalize all these properties to an arbitrary M-cycle with U sequence $U=S_1S_2\cdots S_{M-1}$, $S_i=R$ or L. To define M-furcation, we also need to introduce a complementary sequence $\overline{U}$ by interchanging R and L in U. The U sequence P_n associated with the nth M-furcation is $U(*U)^{n-1}$ which can be expressed iteratively as

$$\begin{aligned}P_{n+1}&=P_n*U\\&\equiv P_nQ_1P_nQ_2\cdots Q_{M-1}P_n\ ,\end{aligned} \tag{2.13}$$

where $Q_i=S_i$ or its complement depending on whether P_n has an even or odd number of R, respectively. We call the original M-cycle with sequence U the basic M-cycle. Given the basic cycle, we obtain all M-furcation sequences trivially.

In fact, all M-furcations converge to Feigenbaum-type fixed points. The parameter a_n associated with the M^n-cycle approaches a limit a_∞ as in Eqs. (2.2) and (2.3). The new universal constant δ is the property of the particular cycle. Analogous to the trifurcation case, iteration and scaling at a_∞ lead to a universal function f^* which obeys the functional relation

$$\alpha f^{*M}(x/\alpha)=f^*(x)\ . \tag{2.14}$$

The scale parameter α is another universal constant which is also the property of the particular cycle.

Perturbing around the fixed-point function f^*, we obtain a linearized equation as in (2.8). Just as in the bifurcation case, all but one of the eigenvalues of Λ have magnitudes smaller than 1. We shall illustrate these properties in a renormalization-group calculation in Sec. IV.

III. NUMERICAL RESULTS OF DIRECT SEARCHES

In this section, we illustrate how to search for the superstable cycles numerically for an S-unimodal map such as

$$x_{n+1}=f(x_n)\equiv 1+ax_n^2 . \tag{3.1}$$

We then obtain the limit point a_∞, the universal constant δ, and α for all M-furcations with $M \le 7$.

By unimodal, we mean that the map is continuous and has a single peak. The function $f(x)$ is increasing on one side of the peak and decreasing on the other side of the peak. For an S-unimodal map, we require further that the Schwarzian derivative of $f(x)$ is everywhere negative. For an S-unimodal map, there is at most one stable cycle, and when such a stable cycle exists, the peak is always in the basin of attraction. Following the images of the peak under repeated mappings, we always approach the attractor. In analogous to a U sequence, we introduce a sequence of R and L according to whether the successive mappings of the peak are on the right or the left of the peak. This sequence is called the kneading sequence of the map. Following the kneading sequence, we can determine whether the map has a stable cycle or not. If such a stable cycle exists, we can determine the U sequence of the stable cycle.

Since there are a large number of M^n cycles for a given M and n, it is important to keep track of the U sequence of the cycle to ensure that the cycle obtained is the correct one. For map such as (3.1), the kneading sequence is properly ordered according to the control parameter $\underline{a}$. Thus, by comparing the kneading sequence associated with an arbitrary parameter $\underline{a}$ and the desired U sequence of a superstable M^n cycle, we can decide whether the parameter $\underline{a}$ is larger or smaller than the desired a_n. We can then increase or decrease the parameter $\underline{a}$ by a proper amount and repeat the search. We have written a program to do this search automatically.

After we obtain the sequence a_n, we can obtain a_∞ and δ via

$$\delta=\lim_{n\to\infty}\left[\frac{a_n-a_{n-1}}{a_{n+1}-a_n}\right], \tag{3.2}$$

$$a_\infty=\lim_{n\to\infty}\left[\frac{a_{n+1}\delta-a_n}{\delta-1}\right]. \tag{3.3}$$

To determine α, we need to iterate $f(x)\equiv 1+a_\infty x^2$ M^n times and obtain

$$\alpha=\lim_{n\to\infty}(\beta_n/\beta_{n+1}) \tag{3.4}$$

with

$$\beta_n\equiv f_n(0) , \tag{3.5}$$

$$f_n(x)\equiv f_{n-1}^M(x)\equiv f^{M\uparrow n}(x) . \tag{3.6}$$

From $f_n(x)$, we can obtain the fixed-point function $f^*(x)$ as

$$f^*(x)=\lim_{n\to\infty}[f_n(x\beta_n)/\beta_n] . \tag{3.7}$$

Note that $f^*(0)=1$, and that $\beta_n\propto\alpha^n$ as $n\to\infty$. Hence, $f^*(x)$ defined here is the same one as described in Sec. II with the desired normalization $f^*(0)=1$. In Table I we present a_∞, α, and δ for all basic M-cycles with $M\le 7$. These exponents represent the exact numerical values.

IV. RENORMALIZATION-GROUP CALCULATION

Self-similarity of $f(x)$ and $f^M(x)$ near the M-furcation limit point is important. It enables us to study the universality behavior of M-furcation from renormalization-group calculations. As mentioned in Sec. III, the M-furcation sequence leads to a fixed-point function $f^*(x)$,

$$f^*(x)=\lim_{n\to\infty}[\alpha^n f^{n\uparrow M}(x/\alpha^n)] .$$

TABLE I. Limit points a_∞ and critical exponents δ and α for all $M\le 7$ Feigenbaum attractors by direct searches of M-furcations in the map $x_{n+1}=1+ax_n^2$.

Basic cycle M	U sequence	M-furcation limit point a_∞	δ	α
2	R	$-1.401\,155\,189$	4.6692	-2.5029
6	RLR^3	$-1.483\,181\,830$	2.1841×10^2	2.0929×10^1
7	RLR^4	$-1.575\,982\,795$	1.4464×10^3	-4.9166×10^1
5	RLR^2	$-1.631\,926\,654$	2.5555×10^2	-2.0128×10^1
7	RLR^2LR	$-1.674\,812\,389$	2.2538×10^3	5.8627×10^1
3	RL	$-1.786\,440\,255$	5.5247×10^1	-9.2773
6	RL^2RL	$-1.781\,216\,806$	2.1841×10^2	2.0929×10^1
7	RL^2RLR	$-1.832\,495\,509$	1.0170×10^4	-1.3137×10^2
5	RL^2R	$-1.862\,224\,022$	1.2871×10^3	4.5804×10^1
7	RL^2R^3	$-1.884\,886\,087$	2.2840×10^2	1.9154×10^2
6	RL^2R^2	$-1.907\,504\,193$	8.5078×10^3	-1.1501×10^2
7	RL^2R^2L	$-1.927\,202\,424$	3.5306×10^4	-2.3009×10^2
4	RL^2	$-1.942\,704\,355$	9.8160×10^2	-3.8819×10^1
7	RL^3RL	$-1.953\,736\,536$	6.3629×10^4	3.1710×10^2
6	RL^3R	$-1.966\,843\,202$	2.8024×10^4	2.0759×10^2
7	RL^3R^2	$-1.977\,191\,407$	1.6716×10^5	-5.0393×10^2
5	RL^3	$-1.985\,539\,529$	1.6931×10^4	-1.6003×10^2
7	RL^4R	$-1.991\,818\,256$	4.8735×10^5	8.5818×10^2
6	RL^4	$-1.996\,383\,246$	2.7913×10^5	-6.4794×10^2
7	RL^5	$-1.999\,096\,124$	4.5120×10^6	-2.6026×10^3

The fixed-point function f^* is self-similar under M iterations,

$$\alpha f^{*M}(x/\alpha)=f^*(x) . \tag{4.1}$$

Just as in the bifurcation case described in Sec. II, we have, in the neighborhood of f^*,

$$f=f^*+\delta f , \tag{4.2}$$

$$f'(x)\equiv \alpha f^M(x/\alpha)=f^*+\delta f' , \tag{4.3}$$

and

$$\delta f'=\Lambda\,\delta f+O((\delta f)^2) , \tag{4.4}$$

where Λ is a linear operator.

In the linear approximation, further M-iterations give

$$f^{(n)}\equiv \alpha f^{(n-1)M}(x/\alpha)=f^*+\delta f^{(n)} \tag{4.5}$$

and

$$\delta f^{(n)}=\Lambda\,\delta f^{(n-1)}=\Lambda^n\delta f . \tag{4.6}$$

It is advantageous to introduce the eigenvectors v_i of Λ,

$$\Lambda v_i=\lambda_i v_i , \tag{4.7}$$

as a set of basis vectors where λ_i are the eigenvalues. Expanding δf as linear combinations of v_i, we have

$$\delta f=\sum_i c_i v_i \tag{4.8}$$

and

$$\delta f^{(n)}=\Lambda^n\delta f=\sum_i c_i\lambda_i^n v_i . \tag{4.9}$$

Discussions given below are well-known in the critical phenomena. The system with all $|\lambda_i|<1$ is noninteresting: All $f(x)$ in the neighborhood of f^* would converge to f^* under M-iterations. The eigenvectors v_i with $|\lambda_i|<1$ are called irrelevant directions. The system with $|\lambda_1|\equiv\delta>1$, but with all other $|\lambda_i|<1$ has a unique nontrivial direction v_1. After a large number of M-iterations and ignoring terms λ_i^n, $i\geq 2$, we have

$$\delta f^{(n)}=c_1\,\delta^n v_1 . \tag{4.10}$$

Thus, all $f(x)$ [or $\delta f(x)$] with the same c_1 but with different c_i, $i\geq 2$ converge to the same iterated function $f^{(n)}(x)$. As we shall see, all our fixed-point functions have only one relevant direction and belong to this category. For maps with a single control parameter a, c_1 is proportional to $a-a_\infty$, and $f^{(n)}(x)$ depends asymptotically only on $(a-a_\infty)\delta^n$. This is the origin of the Feigenbaum universality and the convergence factor δ. The other eigenvalues λ_i $(i\geq 2)$ describe the convergent rate of $f^{(n)}(x)$ to $f^*(x)$ at a_∞.

We are now in a position to carry out the renormalization calculation explicitly. For definiteness, we scale the map of $f(x)$ such that $f(0)=1$. Its M-iterated map after proper scaling is

$$f'(x)=\alpha f^M(x/\alpha) , \tag{4.3}$$

where the scale factor α is chosen to give

$$f'(0)=1 \tag{4.11}$$

or

$$\alpha^{-1}=f^M(0) . \tag{4.12}$$

The universal behavior of an M-furcation sequence is associated with the fixed point of (4.3), namely,

$$f^*(x)=\alpha f^{*M}(x/\alpha) . \tag{4.1}$$

To describe the functional dependence of (4.3), we need to parametrize $f(x)$ and $f'(x)$ in (4.3) by a set of coefficients. Since the maps are self-similar near the peak $x=0$, we use the Taylor-expansion coefficients as the parametrization coefficients. In the following, we shall restrict ourselves to even functions

$$f(x)=1+a_1x^2+a_2x^4+a_3x^6+\cdots \tag{4.13}$$

and

$$f'(x)=1+a_1'x^2+a_2'x^4+a_3'x^6+\cdots . \tag{4.14}$$

Equation (4.3) determines coefficients $\{a_i'\}$ as functions of $\{a_i\}$.

In an actual calculation, we cannot keep an infinite set of coefficients. We need to make some truncation. In this paper, we keep only three coefficients a_1, a_2, and a_3, and ignore terms x^8 and higher. As we shall see, this approximation gives very satisfactory results.

To obtain $\{a_n'\}$, we need to evaluate $f^M(x)$. We can accomplish this by repeated applications of

$$f(g(x))=1+a_1[g(x)]^2+a_2[g(x)]^4+a_3[g(x)]^6 \tag{4.15}$$

with $g(x)$ being $f(x), f^2(x), \ldots, f^{M-1}(x)$, respectively. Knowing the coefficients of $g(x)$ as

$$g(x)=b_0+b_1x^2+b_2x^4+b_3x^6+\cdots , \tag{4.16}$$

we can use (4.15) to obtain the coefficients of $f(g(x))$. We have described an algorithm for computing these truncated coefficients explicitly in Appendix A. With the help of a computer, we can work out the coefficients of $f^M(x)$ and consequently those of $f'(x)$.

In terms of the coefficient relations

$$a_i'=f_i(a_1,a_2,a_3),\quad i=1,2,3 \tag{4.17}$$

we can express the fixed-point condition (4.1) as

$$a_i^*=f_i(a_1^*,a_2^*,a_3^*) . \tag{4.18}$$

For a given M, there are many fixed-point solutions. However, we are able to reach the desired fixed points by Newton's method starting from $f=1+a_\infty x^2$.

In the neighborhood of a_i^*, we can expand $\delta a_i' \equiv a_i'-a_i^*$ as linear combinations of $\delta a_i\equiv a_i-a_i^*$, giving

$$\delta a_i'=\frac{\partial f_i}{\partial a_j}\delta a_j+O((\delta a)^2) . \tag{4.19}$$

By diagonalizing the matrix $\partial f_i/\partial a_j$, we obtain three eigenvalues λ_1, λ_2, and λ_3. It is pleasing to see that, for all fixed points that we have studied, only one (chosen as λ_1) of the three eigenvalues is larger than 1. We can identify this relevant eigenvalue as δ. The fact that we only have

TABLE II. A summary of all $M \leq 7$ Feigenbaum fixed-point functions $f^*(x) \equiv 1 + a_1^* x^2 + a_2^* x^4 + a_3^* x^6 + \cdots$ and their associated eigenvalues λ_i based on three-parameter renormalization-group calculation.

Basic cycle M	U sequence	a_1^*	Coefficients of $f^*(x)$ a_2^*	a_3^*	Scale factor α	$\delta \equiv \lambda_1$	Associated eigenvalues λ_2	λ_3
2	R	$-1.521\,843$	$7.293\,158 \times 10^{-2}$	$4.550\,859 \times 10^{-2}$	-2.4789	4.5165	5.0997×10^{-1}	-8.9015×10^{-2}
6	RLR^3	$-1.515\,767$	$3.155\,801 \times 10^{-2}$	$2.495\,466 \times 10^{-3}$	2.0927×10^{1}	2.1836×10^{2}	1.2557×10^{-2}	2.6548×10^{-3}
7	RLR^4	$-1.568\,313$	$-8.845\,720 \times 10^{-3}$	$5.103\,342 \times 10^{-4}$	-4.9166×10^{1}	1.4464×10^{3}	-1.2742×10^{-2}	3.9538×10^{-4}
5	RLR^2	$-1.623\,952$	$-1.171\,178 \times 10^{-2}$	$3.157\,520 \times 10^{-3}$	-2.0127×10^{1}	2.5549×10^{2}	-3.6958×10^{-2}	2.3154×10^{-3}
7	RLR^2LR	$-1.675\,089$	$-1.084\,651 \times 10^{-4}$	$4.338\,662 \times 10^{-4}$	5.8627×10^{1}	2.2538×10^{3}	1.5055×10^{-3}	2.9164×10^{-4}
3	RL	$-1.874\,349$	$9.382\,053 \times 10^{-2}$	$-2.432\,021 \times 10^{-4}$	-9.2764	5.5233×10^{1}	1.8276×10^{-2}	-6.6929×10^{-2}
6	RL^2RL	$-2.113\,988$	$3.431\,687 \times 10^{-1}$	$1.256\,338 \times 10^{-2}$	2.0819×10^{1}	2.1571×10^{2}	1.0320×10^{-2}	$\pm i \times 5.2755 \times 10^{-3}$
7	RL^2RLR	$-1.833\,086$	$5.537\,179 \times 10^{-4}$	$7.682\,142 \times 10^{-5}$	-1.3137×10^{2}	1.0170×10^{4}	-2.3555×10^{-3}	5.8087×10^{-5}
5	RL^2R	$-1.872\,732$	$1.062\,060 \times 10^{-2}$	$5.071\,018 \times 10^{-4}$	4.5804×10^{1}	1.2870×10^{3}	5.6421×10^{-3}	5.0623×10^{-4}
7	RL^2R^3	$-1.886\,017$	$1.160\,742 \times 10^{-3}$	$3.402\,792 \times 10^{-5}$	1.9154×10^{2}	2.2840×10^{4}	1.9629×10^{-3}	2.7396×10^{-5}
6	RL^2R^2	$-1.908\,799$	$-1.276\,451 \times 10^{-3}$	$9.432\,325 \times 10^{-5}$	-1.1501×10^{2}	8.5078×10^{3}	-5.3122×10^{-3}	7.6015×10^{-5}
7	RL^2R^2L	$-1.925\,824$	$1.482\,433 \times 10^{-3}$	$3.523\,238 \times 10^{-5}$	-2.3099×10^{2}	3.5306×10^{4}	-5.2190×10^{-3}	1.8781×10^{-5}
4	RL^2	$-1.971\,404$	$2.998\,511 \times 10^{-2}$	$1.341\,579 \times 10^{-4}$	-3.8819×10^{1}	9.8160×10^{2}	-6.3541×10^{-3}	7.4402×10^{-4}
7	RL^3RL	$-1.955\,168$	$1.463\,911 \times 10^{-3}$	$1.496\,678 \times 10^{-5}$	3.1710×10^{2}	6.3629×10^{4}	3.0218×10^{-3}	1.0003×10^{-5}
6	RL^3R	$-1.968\,929$	$2.166\,983 \times 10^{-3}$	$2.622\,023 \times 10^{-5}$	2.0759×10^{2}	2.8024×10^{4}	1.6914×10^{-3}	2.3519×10^{-5}
7	RL^3R^2	$-1.977\,639$	$4.534\,021 \times 10^{-4}$	$4.971\,406 \times 10^{-6}$	-5.0393×10^{2}	1.6716×10^{5}	-9.5078×10^{-4}	3.9481×10^{-6}
5	RL^3	$-1.993\,189$	$7.785\,471 \times 10^{-3}$	$-1.036\,348 \times 10^{-5}$	-1.6003×10^{2}	1.6931×10^{4}	1.9823×10^{-3}	3.9941×10^{-5}
7	RL^4R	$-1.992\,314$	$4.988\,842 \times 10^{-4}$	$1.557\,910 \times 10^{-6}$	8.5818×10^{2}	4.8735×10^{5}	5.8826×10^{-4}	1.3623×10^{-6}
5	RL^4R	$-1.998\,326$	$1.954\,581 \times 10^{-3}$	$-6.721\,242 \times 10^{-7}$	-6.4794×10^{2}	2.7913×10^{5}	1.4353×10^{-3}	2.3959×10^{-6}
7	RL^5	$-1.999\,584$	$4.885\,655 \times 10^{-4}$	$-4.228\,151 \times 10^{-8}$	-2.6026×10^{3}	4.5120×10^{6}	5.9880×10^{-4}	1.4785×10^{-7}

one relevant eigenvalue is responsible for the universality behavior of M-furcation fixed points. In Table II, we present for all $M \leq 7$ cycles the numerical results of $\{a_i^*\}$, α, and δ. These exponents are only approximate because we have truncated the Taylor series to include x^6 or lower terms.

V. FRACTAL DIMENSIONS

It is known that the basin of attraction associated with a Feigenbaum fixed point forms a Cantor set. In the following, we shall describe briefly how to construct this Cantor set geometrically.[13] This construction provides us with a method for computing the fractal dimensions efficiently.[14]

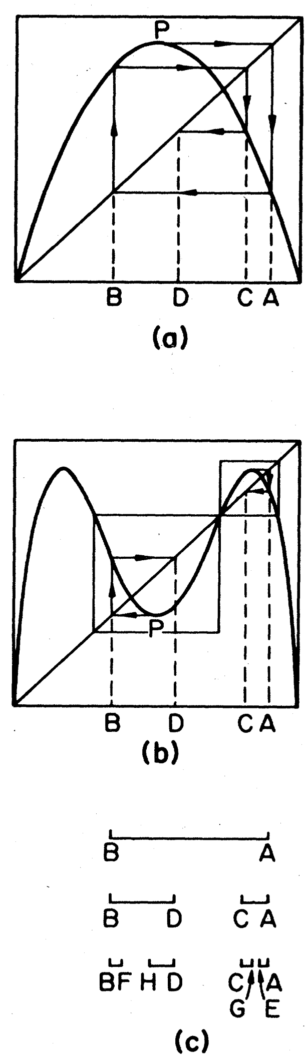

FIG. 3. (a) Iterative images of the peak P. All points inside the box but outside the interval BA will eventually map into BA. (b) Map f^2 consists of two independent small boxes which map into themselves. Inside these boxes, all points will eventually map into intervals BD and CA. (c) By removing the regions in which the attractor does not reside, we arrive at a geometrical construction of a Cantor set.

Consider an $f(x)$ obtained as the bifurcation limit of 2^n cycles. For the simplest quadratic map, this Feigenbaum limit map is given by

$$x_{n+1}=f(x_n)\equiv 1+a_\infty x_n^2$$

with $a_\infty=-1.401\,155$. For x lying in the interval $(-1.273\,929, 1.273\,929)$, $f(x)$ will remain in the above interval. In Fig. 3(a), we have plotted this $f(x)$. The simplest way to describe the attractor is to follow the itinerary of the peak at $x=0$: $P\to A\to B\to C\to D\to\cdots$ where $A,B,C,\ldots$ denote $f(0), f^2(0), f^3(0),\ldots$. It is easy to see that all points inside the interval $(-1.273\,929, 1.273\,929)$ but outside the line interval BA will eventually map into the interval BA. Thus, the attractor must lie in the closed interval BA.

Next, we note that $f^2(x)$ has the same basin of attraction as that of $f(x)$. We have plotted $f^2(x)$ in Fig. 3(b). The $f^2(x)$ map consists of two disjoint single-hump maps as denoted in the smaller boxes. The maps inside these boxes are analogous to the original map $f(x)$. Thus we conclude that the attractor must lie inside two disjoint intervals BD and CA. We may construct these two subintervals by removing DC from BA. This procedure is precisely the geometric construction of a Cantor set.

In our Cantor set, the ratios $BF:FH:HD$ and $CG:GE:EA$ are not the same. Thus the Cantor set that we have constructed is not exactly self-similar. Numerically, we find that the deviation of our Cantor set from a self-similar Cantor set is small.

It is easy to obtain the capacity dimensions d_c and the information dimension d_I for a self-similar Cantor set.[15] Consider a Cantor set constructed as follows: We first delete portions of the interval [0,1] to give n subintervals of lengths $q_1, q_2, \ldots, q_n$. Next, we delete the same fractions of intervals out of each of the intervals $q_1, q_2, \ldots, q_n$. Repeating this construction, we obtain as a limit a self-similar Cantor set. The capacity dimension d_c for this Cantor set is given by

$$\sum_{a=1}^{n} q_a^{d_c}=1\,. \tag{5.1}$$

To determine the information dimension d_I, we also need to know the relative probability p_i of the attractor to be in the subinterval q_i. If p_i is the same in each level of its construction, the information dimension is given by

$$d_I=\frac{\sum_a p_a \ln(1/p_a)}{\sum_a p_a \ln(1/q_a)}\,. \tag{5.2}$$

It is important to point out that we can apply Eqs. (5.1) and (5.2) to a self-similar Cantor set at any stage of its construction and obtain the same results. For completeness, we include a simple derivation of these formulas in Appendix B.

In an actual calculation, we first iterate $f(x)$ at a_∞ to obtain the universal function $f^*(x)$. We then apply the geometrical construction method discussed earlier to obtain the Cantor set. By treating these subintervals at various levels as the beginning of a self-similar Cantor set, we

TABLE III. Calculation of fractal dimensions for a Feigenbaum attractor approximated by self-similar Cantor sets.

No. of initial subintervals ($\equiv 2^n$)	$d_c(n)$	$nd_c(n)-(n-1)d_c(n-1)$	$d_I(n)$	$nd_I(n)-(n-1)d_I(n-1)$
4	0.537 474 6		0.517 300 4	
8	0.537 688 3	0.538 116	0.517 274 7	0.517 223
16	0.537 772 2	0.538 024	0.517 219 2	0.517 053
32	0.537 827 5	0.538 049	0.517 195 0	0.517 098
64	0.537 863 7	0.538 045	0.517 178 7	0.517 097

can compute the approximate information and capacity dimensions of this Cantor set.[16] In Table III, we have shown the numerical results associated with Feigenbaum bifurcation attractor. As we can see, the self-similarity assumption becomes better as one increases the number of initial subintervals. The difference between $d_c(n)$ [or $d_I(n)$] and $d_c(\infty)$ is approximately proportional to $1/n$. The expression $nd_c(x)-(n-1)d_c(n-1)$ converges to $d_c(\infty)$ very rapidly. We thus obtain

$$d_c = 0.538\,045\ ,$$

$$d_I = 0.517\,097\ .$$

These numbers agree with those obtained earlier by Grassberger.[17]

We can generalize the method to M-furcations easily. We have summarized the capacity and information dimensions associated with all $M \leq 7$ M-furcation attractors in Table IV.

TABLE IV. Fractal dimensions for all $M \leq 7$ Feigenbaum attractors.

Basic cycle	U sequence	d_I	d_c
2	R	0.5171	0.5380
6	RLR^3	0.4036	0.4209
7	RLR^4	0.3425	0.3577
5	RLR^2	0.3676	0.3835
7	RLR^2LR	0.3254	0.3398
3	RL	0.3354	0.3500
6	RL^2RL	0.4036	0.4209
7	RL^2RLR	0.2732	0.2858
5	RL^2R	0.2894	0.3029
7	RL^2R^3	0.2560	0.2682
6	RL^2R^2	0.2610	0.2735
7	RL^2R^2L	0.2448	0.2561
4	RL^2	0.2567	0.2689
7	RL^3RL	0.2314	0.2423
6	RL^3R	0.2316	0.2434
7	RL^3R^2	0.2167	0.2280
5	RL^3	0.2145	0.2253
7	RL^4R	0.1987	0.2094
6	RL^4	0.1870	0.1968
7	RL^5	0.1670	0.1760

VI. DISCUSSION

In this paper, we have studied the M-furcations for single-hump one-dimensional maps. In order to study M-furcations, we need an efficient algorithm for determining the locations of all superstable cycles. We find that the most reliable algorithm is to follow the itinerary of the peak. By comparing the itinerary with the desired U sequence, we know immediately whether we should increase or decrease the control parameter in order to reach the required superstable cycle. For a map such as

$$x_{n+1} = 1 + ax_n^2\ ,$$

we may begin at $a=-1$, and modify $\underline{a}$ by $\pm 1/2, \pm 1/4, \pm 1/8, \ldots,$ successively. The parameter $\underline{a}$ converges rapidly to the desired limit. Knowing $\{a_n\}$, we can obtain the universal constants δ and α and the fixed-point function $f^*(x)$ easily.

We have also studied the universal behavior through renormalization-group calculations. The renormalization-group calculation helps us understand why the Feigenbaum universal behavior works so well. Even though we use only three parameters in our calculation, the agreement between the renormalization-group calculation and the direct search is already remarkable. It is pleasing to see that there is only one relevant eigenvalue ($|\lambda_1| \equiv \delta > 1$) for each of the M-furcation fixed points. It is also interesting to note that for the majority of the fixed points, the relevant eigenvalues are large ($\sim 10^4$) and their irrelevant eigenvalues are small (10^{-2} or smaller). This makes a complete dominance of the relevant eigenvectors after one or two M-fold iterations.

We have computed the fractal dimensions d_c and d_I numerically by approximating the attractors with self-similar Cantor sets. There are several modifications which may increase the convergence and the accuracy of our fractal dimension calculation. It is easy to verify that our attractors are not exactly self-similar. For instance, in the bifurcation case, one sees immediately that half of the sub-Cantor set (subset BD in Fig. 3) is similar to the original set. The other half (subset CA in Fig. 3) is related to the original set by a monotonic, nonlinear transformation. If we approximate this nonlinear transformation by a linear one, we obtain a self-similar Cantor set. On the other hand, if we approximate the nonlinear transformation by a sequence of linear segments, we arrive at some quasisimilar Cantor set. We can derive equations for d_I

and d_c for these quasisimilar Cantor sets. These equations are more complicated than Eqs. (5.1) and (5.2), but are more accurate for any given order of iterations. Thus, for a given amount of computing time, there is a trade-off between using lower-order accurate description of a quasisimilar Cantor set versus the higher-order self-similar Cantor set.

The fractal dimensions have important physical significance. They describe the repetitions of the structure in finer scales. One possible application is to relate the fractal behavior of an attractor to its power spectrum.[18] The N-furcation attractor and its fractal dimensions may provide useful information about the power spectra of its Nth harmonics.

Since self-similarity is the underlying basis of our calculation, we believe that one should be able to compute d_c and d_I analytically through a renormalization-group calculation. At the moment, we do not know how to formulate the problem yet.

As we have mentioned in the Introduction, there are significant similarities between the onset of turbulence in fluid and the transition to chaos in one-dimensional maps. It is our hope that a thorough study of this simple one-dimensional system may teach us valuable lessons about how to handle the real turbulence problem in the future.

ACKNOWLEDGMENTS

We wish to thank Professor A. Jackson for stimulating discussions, Professor J. Wright for developing an algorithm as described in Appendix A, and Professor P. Grassberger for useful comments and for communicating to us a precise unpublished value of d_c. We thank the Research Board of the University of Illinois for providing us with some free computer time. This work was supported in part by the National Science Foundation under Grant No. PHY-82-01948.

APPENDIX A: ALGORITHM FOR COMPUTING TRUNCATED COEFFICIENTS

In this appendix, we describe an algorithm for computing systematically the truncated coefficients of $f^M(x)$. This method was developed by Wright during the collaboration of Wortis, Wright, and one of the present authors (S.J.C.) in an earlier research.

Consider a one-dimensional map

$$f(x)=1+a_1x^2+a_2x^4+a_3x^6 . \tag{A1}$$

Our goal is to compute $f^M(x)$ by keeping terms up to x^6. One way to do the calculation is to evaluate $f^M(x)$ to all orders, and truncate the result to the x^6 term after the calculation. This is a very tedious method, and it becomes impractical to perform for M larger than 3 or 4.

Fortunately, there is a way to compute these truncated coefficients by keeping terms up to x^6 in the intermediate calculation. Assume that $f(x)$ in Eq. (A1) is exact and that an intermediate expression $g(x)$ is known up to x^6 terms

$$g(x)=b_0+b_1x^2+b_2x^4+b_3x^6+\cdots . \tag{A2}$$

If we replace x in Eq. (A1) by $g(x)$ and keep terms of x^6 and lower, we have

$$\begin{aligned} f(g(x))&=1+a_1[g(x)]^2+a_2[g(x)]^4+a_3[g(x)]^6 \\ &=c_0+c_1x^2+c_2x^4+c_3x^6+\cdots . \end{aligned} \tag{A3}$$

It is easy to see that the truncated terms in $g(x)$ do *not* contribute to the coefficients c_0, c_1, c_2, and c_3. For expansions up to x^6 terms, we can compute these coefficients exactly as

$$c_0=1+a_1b_0^2+a_2b_0^4+a_3b_0^6 , \tag{A4}$$

$$c_1=2a_1b_0b_1+4a_2b_0^3b_1+6a_3b_0^5b_1 , \tag{A5}$$

$$\begin{aligned} c_2=&\, a_1(2b_0b_2+b_1^2)+a_2(6b_0^2b_1^2+4b_0^3b_2) \\ &+a_3(15b_0^4b_1^2+6b_0^5b_2) , \end{aligned} \tag{A6}$$

$$\begin{aligned} c_3=&\, a_1(2b_0b_3+2b_1b_2)+a_2(12b_0^2b_1b_2+4b_0^3b_3+4b_1^3) \\ &+a_3(30b_0^4b_1b_2+6b_0^5b_3+20b_1^3) . \end{aligned} \tag{A7}$$

We can apply Eqs. (A3)—(A7) repeatedly without introducing any error in the new coefficients. In particular, we can obtain the coefficients of $f^M(x)$ by repeated applications of (A3)—(A7) to

$$\begin{aligned} &f^2(x)=f(f(x)) , \\ &f^3(x)=f(f^2(x)) , \end{aligned} \tag{A8}$$

etc. After obtaining $f^M(x)$, we make a scale transformation

$$f'(x)=\beta f^M(x/\beta) \tag{A9}$$

with

$$\beta^{-1}=f^M(0) . \tag{A10}$$

The new function $f'(x)$ obeys the proper normalization $f'(0)=1$, and has the desired series expansion

$$f'(x)=1+a_1'x^2+a_2'x^4+a_3'x^6+\cdots . \tag{A11}$$

Coefficients a_i' are the input of our renormalization-group calculation described in Sec. IV. [See, e.g., Eq. (4.17).]

We can generalize our method to an arbitrary x^n truncation, and to functions of several variables.

APPENDIX B: FRACTAL DIMENSIONS FOR A SELF-SIMILAR CANTOR SET

A self-similar Cantor set S is a set whose subsets are similar to the original set. Consider an interval [0,1] with unit length. We remove part of the line segment, and arrive at n disconnected subintervals $(q_1,q_2,\ldots,q_n)$. If we continue to remove part of the subintervals, and make these subsets all similar to the original set S, then the final construction is a self-similar Cantor set. Let $(S_1,S_2,\ldots,S_n)$ be the subsets associated with the subintervals $(q_1,q_2,\ldots,q_n)$. Then

$$S=\bigcup_{i=1}^{n} S_i \tag{B1}$$

and each S_i is identical to S up to a scaling factor. We can use the self-similarity property of S to determine its fractal dimensions.

To measure the capacity dimension d_c, we count the number of ϵ-size boxes which the attractor visits, and obtain

$$d_c=\lim_{\epsilon\to 0}\left[\frac{\ln N(\epsilon)}{\ln(1/\epsilon)}\right] . \tag{B2}$$

We can rewrite (B2) as

$$N(\epsilon)=A(\epsilon)\left[\frac{1}{\epsilon}\right]^{d_c} , \tag{B3}$$

where coefficient A may have a mild ϵ dependence such as step functions or $[\ln(1/\epsilon)]^{\alpha}$. To give a well-defined d_c, it is only necessary to have $\ln A/\ln(1/\epsilon)=0$ as $\epsilon\to 0$. In our case, A is actually bounded from both above and below.

We can use the self-similarity property of S to obtain the number of boxes in a subset S_i associated with the interval q_i:

$$N_i=A(\epsilon/q_i)\left[\frac{q_i}{\epsilon}\right]^{d_c} . \tag{B4}$$

Since $N=\sum N_i$, we have

$$A(\epsilon)\left[\frac{1}{\epsilon}\right]^{d_c}=\sum_i A(\epsilon/q_i)\left[\frac{q_i}{\epsilon}\right]^{d_c} . \tag{B5}$$

The $(1/\epsilon)^{d_c}$ factors cancel. By considering the limit $\epsilon\to 0$ with $A(\epsilon)$ approaching its upper and its lower bounds separately, we prove easily that

$$\sum_i q_i^{d_c}=1 . \tag{B6}$$

This is the required equation for d_c.

To obtain the information dimension d_I, we need to know the probability distribution for finding the attractor in each of the subintervals q_i. We assume that the relative probability of the attractor in subinterval q_i is p_i and that the same relative probability holds for further partitions of the subsystems. In our problem, our p_i's are equal to $1/n$.

In terms of box counting, we may define the information dimension d_I as

$$d_I=\lim_{\epsilon\to 0}\left[\frac{\sum_a p_a \ln(1/p_a)}{\ln(1/\epsilon)}\right] . \tag{B7}$$

Index $\underline{a}$ runs over boxes which the attractor visits, and p_a is the probability for the attractor to be in box $\underline{a}$. In analogy to our previous result, we may rewrite (B7) as

$$I(\epsilon)\equiv\sum_a p_a \ln(1/p_a)=d_I \ln(1/\epsilon)+B(\epsilon) , \tag{B8}$$

where $B/\ln(1/\epsilon)\to 0$ as $\epsilon\to 0$. In our case, the additive term $B(\epsilon)$ is bounded from both above and below.

We consider the index $\underline{a}$ as the direct sum of n indices $(a_1,a_2,\ldots,a_n)$ which run over boxes in the subintervals $(q_1,q_2,\ldots,q_n)$. For $\underline{a}$ in the ith subinterval, we write

$$p_a=p_i p_{ai} , \tag{B9}$$

where p_{ai} is the relative probability of finding the attractor in the a_ith box knowing that is is in the ith interval. Probability p_{ai} obeys the normalization

$$\sum_{a,i} p_{ai}=1 . \tag{B10}$$

Using the self-similarity property, we can introduce I_i associated with the ith subinterval as

$$\begin{aligned} I_i(\epsilon/q_i)&\equiv\sum_{a,i} p_{ai}\ln(1/p_{ai}) \\ &=d_I \ln(q_i/\epsilon)+B(\epsilon/q_i) . \end{aligned} \tag{B11}$$

Using (B9) and (B11), we can relate $I(\epsilon)$ and $I_i(\epsilon/q_i)$ as

$$\begin{aligned} I(\epsilon)&=d_I \ln(1/\epsilon)+B(\epsilon) \\ &=\sum_a p_a \ln(1/p_a) \\ &=\sum_i \sum_{a,i} p_i p_{ai}[\ln(1/p_i)+\ln(1/p_{ai})] \\ &=\sum_i p_i \ln(1/p_i)+\sum_i p_i I_i(\epsilon/q_i) \\ &=\sum_i p_i \ln(1/p_i)+\sum_i p_i[d_I \ln(q_i/\epsilon)+B(\epsilon/q_i)] . \end{aligned} \tag{B12}$$

The $\ln(1/\epsilon)$ terms in (B12) cancel, and we obtain

$$\sum_i p_i \ln(1/p_i)+d_I\sum_i p_i \ln q_i=B(\epsilon)-\sum_i p_i B(\epsilon/q_i) . \tag{B13}$$

By considering the limit $\epsilon\to 0$ with $B(\epsilon)$ approaching its upper and lower bounds separately, we arrive at

$$\sum_i p_i \ln(1/p_i)+d_I\sum_i p_i \ln q_i=0 \tag{B14}$$

or

$$d_I=\frac{\sum_i p_i \ln(1/p_i)}{\sum_i p_i \ln(1/q_i)} . \tag{B15}$$

Equation (B15) is the desired equation of d_I for a self-similar Cantor set.

---

*Present address: Physics Department, Princeton University, Princeton, NJ 08544.

[1]R. M. May, Nature (London) **261**, 459 (1976).

[2]P. Collet and J. P. Eckmann, *Iterated Maps on the Interval as Dynamics Systems* (Birkhäuser, Boston, Mass., 1980).

[3]M. J. Feigenbaum, J. Stat. Phys. **19**, 25 (1978); **21**, 7 (1979). See also M. J. Feigenbaum, Los Alamos Sci. **1**, 4 (1980).

[4]A one-dimensional map with more than one peak may develop

richer phase-transition phenomena such as tricritical points. See, S. J. Chang, M. Wortis, and J. A. Wright, Phys. Rev. A **24**, 2669 (1981).

[5]Iterative equations appear in the real space renormalization group treatment of spin systems. They also appear in incommensurate and/or commensurate transitions.

[6]The Lorenz model is a three-parameter truncation of the Navier-Stokes equation. Effective one-dimensional iterative maps and bifurcations emerge naturally in the Lorenz model. See, e.g., E. N. Lorenz, J. At. Sci. **20**, 130 (1963). See also the review articles: J. P. Eckmann, Rev. Mod. Phys. **53**, 643 (1981); E. Ott, *ibid.* **53**, 655 (1981). Bifurcation and similar behavior also appear in a five-parameter truncation of the Navier-Stokes system: V. Franceschini and C. Tebaldi, J. Stat. Phys. **21**, 707 (1979).

[7]See the proceedings of the Beam-Beam Interaction Seminar held at Stanford Linear Accelerator Center, Stanford, California, May 1980, Stamford Linear Accelerator Center Report No. SLAC-PUB-2624, Conf-8005102 (unpublished).

[8]See, e.g., U. Frisch and P.-L. Sulem, J. Fluid Mech. **87**, 719 (1978); A. J. Chorin, J. Comput. Phys. **46**, 390 (1982).

[9]S. J. Chang and J. McCown, Phys. Rev. A **30**, 1149 (1984).

[10]N. Metropolis, M. L. Stein, and P. R. Stein, J. Comb. Theor. **15**, 25 (1973).

[11]We use the work "bifurcation" to describe the period-doubling bifurcation.

[12]B. Derrida, A. Gervois, and Y. Pomeau, J. Phys. A **12**, 269 (1969). These authors introduced the inner composition law ($*$ product).

[13]This method of determining a Feigenbaum attractor has been described earlier by J. P. Crutchfield *et al.*, Phys. Rep. **92**, 45 (1982).

[14]For reviews on fractal dimensions, see, e.g., J. D. Farmer, E. Ott, and J. A. Yorke, Physica D **7**, 153 (1983); J. D. Farmer, in *Evolution of Order and Chaos,* edited by H. Haken (Springer, Berlin 1982).

[15]Both the capacity dimension d_c and the information dimension d_I studied in this paper can in principle be obtained by the box counting method. See Ref. 14 for their definition.

[16]Obviously, considering this Cantor set as generated by 2^n intervals with increasing n will not make the final Cantor set any more self-similar. Nevertheless, this treatment does lead to increasingly more accurate values of d_c and d_I. A more accurate treatment is to consider the Cantor set as quasi-self-similar, as described in the Discussion (Sec. VI).

[17]P. Grassberger, J. Stat. Phys. **26**, 173 (1981); P. Grassberger and I. Procaccia, Physica D **9**, 189 (1983); P. Grassberger (private communication).

[18]See, e.g., J. D. Farmer, Phys. Rev. Lett. **47**, 179 (1981).